LUND UNIVERSITY
Faculty of Medicine

LUP

Lund University Publications
Institutional Repository of Lund University

This is an author produced version of a paper published in Cell metabolism. This paper has been peer-reviewed but does not include the final publisher proof-corrections or journal pagination.

Citation for the published paper:

Dai-Qing Li, Xing-Jun Jing, S Albert Salehi, Stephan C Collins, Michael B Hoppa, Anders Rosengren, Enming Zhang, Ingmar Lundquist, Charlotta Olofsson, Matthias Mörgelin, Lena Eliasson, Patrik Rorsman, Erik Renström

"Suppression of sulfonylurea- and glucose-induced insulin secretion in vitro and in vivo in mice lacking the chloride transport protein ClC-3."

Cell metabolism, 2009, 10 (4) 309 - 315

http://dx.doi.org/10.1016/j.cmet.2009.08.011

Access to the published version may require journal subscription.
Published with permission from: Elsevier

* [C] Manuscript
Click here to view linked References

Suppression of sulfonylurea- and glucose-induced insulin secretion in vitro and in vivo in mice lacking the chloride transport protein ClC-3

Dai-Qing Li[1,2], Xingjun Jing[1], Albert Salehi[1], Stephan C. Collins[3], Michael B. Hoppa[3], Anders H. Rosengren[1], Enming Zhang[1] Ingmar Lundquist[1], Charlotta S. Olofsson[4], Matthias Mörgelin[5], Lena Eliasson[1], Patrik Rorsman[3], Erik Renström[1+]

[1]Lund University Diabetes Center, Department of Clinical Sciences Malmö, Lund University, Malmo University Hospital entrance 72, CRC 91-11, SE-205 02 Malmö, Sweden
[2] Key lab of Hormones and Development, Ministry of Health, China, Tianjin Metabolic Diseases Hospital, Tianjin Medical University, China.
[3] Oxford Centre for Diabetes, Endocrinology and Metabolism, University of Oxford, Oxford OX3 7LJ, UK.
[4] Department of Physiology, Göteborg University, Medicinaregatan 11, Box 432, SE-405 30 Göteborg, Sweden.
[5]Department of Clinical Sciences Lund, Division of Infection Medicine, Lund University, BMC, B14, SE-221 84 Lund, Sweden.

[+]To whom correspondence should be addressed

Contact:
Erik Renström:
Phone: +46-40-39 11 57
Fax: +46-40-39 12 22
e-mail: erik.renstrom@med.lu.se

Nonstandard abbreviations used:

KO, knock-out; WT, wildtype; RRP, readily releasable pool; LDCV, large dense-core vesicle; SLMV, synaptic-like microvesicle

Running title: Ablation of CLC3 suppresses insulin secretion

SUMMARY

Priming of insulin secretory granules for release requires intragranular acidification and depends on vesicular Cl^--fluxes, but the identity of the chloride transporter/ion channel involved is unknown. We tested the hypothesis that the chloride transport protein ClC-3 fulfills these actions in pancreatic β-cells. In $ClC3^{-/-}$ mice, insulin secretion evoked by membrane depolarization (high extracellular K^+, sulfonylureas) or glucose was >60% reduced compared to wildtype animals. This effect was mirrored by a ~80% reduction in depolarization-evoked β-cell exocytosis (monitored as increases in cell capacitance) in single $ClC3^{-/-}$ β-cells, as well as a 44% reduction in proton transport across the granule membrane. ClC-3 expression in the insulin granule was demonstrated by immunoblotting, immunostaining and negative immuno electronmicroscopy in a high-purification fraction of LDCVs obtained by phogrin-EGFP labelling. The data establish the importance of granular Cl^- fluxes in granule priming and provide direct evidence for the involvement of ClC-3 in the process.

INTRODUCTION

A low intragranular pH is crucial for prohormone cleavage in pancreatic β-cells (Hutton, 1989). In addition, the acidification of secretory vesicles may play a role in making them release-competent, an ATP-dependent process referred to as priming (Barg et al., 2001; Rorsman and Renstrom, 2003). Acidification is carried out by a V-type H^+-ATPase that pumps H^+ into the vesicular lumen. Without charge compensation, this electrogenic process leads to a lumen-positive voltage across the granular membrane that would prevent further proton pumping. Acidic organelles of the endosomal pathway principally depend on Cl^- fluxes for charge neutralization (al-Awqati, 1995; Sonawane and Verkman, 2003). Consistent with such a mechanism, procedures inhibiting transmembrane Cl^- fluxes in β-cell granules impair their luminal acidification and their priming for exocytosis (Barg et al., 2001).

Various members of the ClC family of Cl^- transport proteins facilitate the acidification of intracellular vesicles (Hara-Chikuma et al., 2005; Piwon et al., 2000; Stobrawa et al., 2001). ClC-3 is present on endosomes and synaptic vesicles (Salazar et al., 2004; Stobrawa et al., 2001) and acidification rates in both types of vesicle were reduced in ClC-$3^{-/-}$ mice (Stobrawa et al., 2001; Yoshikawa et al., 2002). In addition, ClC-3 has also been proposed to be present in β-cell secretory granules (Barg et al., 2001). Functional experiments indicate that ClC-3 facilitates insulin secretion by enhancing the acidification of insulin-containing granules (Barg et al., 2001; Juhl et al., 2003). Here we have addressed this possibility using constitutive ClC-3 knock-out (KO) mice.

RESULTS

ClC-3-dependence of insulin processing and secretion

Insulin secretion was measured in static batch incubations (Fig. 1A). In wildtype islets, the sulfononylurea glibenclamide (2 μM) and high extracellular K^+ (50 mM) stimulated insulin secretion 3.1- and 3.4-fold over basal. Glucose (20 mM) was a much stronger secretagogue and resulted in a ~10-fold stimulation; the latter effect being enhanced 1.8-fold by glucagon-like peptide 1 (100 nM; GLP-1). In ClC-3-deficient (ClC-$3^{-/-}$) islets, the stimulatory effects of glibenclamide and high K^+ were abolished whereas the stimulatory effect of glucose was reduced by 67%. GLP-1 remained stimulatory (179±21%; $P<0.01$) in ClC-$3^{-/-}$ islets, but secretion was nevertheless reduced by 57% relative to wildtype values. We then investigated the possible effect of ClC-3 on proinsulin processing in a subset of the experiments (Fig. 1C). In both wildtype and ClC-$3^{-/-}$ islets, proinsulin secretion was barely detectable under basal conditions (1 mM glucose). Also in high glucose (20 mM), release of mature insulin strongly dominated (>98%) over that of proinsulin. Although the molar ratio of insulin/proinsulin release was significantly lower in ClC-$3^{-/-}$ islets compared to wildtype (Fig. 1D), these data show that the strong secretion defect of the ClC-$3^{-/-}$ islets cannot be attributed to impaired insulin processing. In agreement with this conclusion, insulin content was only reduced by only ~10% in ClC-$3^{-/-}$ islets (Fig. 1B). Although pancreatic α-cells also express ClC-3 (Maritzen et al., 2008), glucagon secretion was unaffected by ablation of ClC-3 (Supplemental Fig. 1).

Ca^{2+} homeostasis is unaffected by ClC-3 ablation

Glucose stimulates insulin secretion by induction of Ca^{2+}-dependent electrical activity that triggers exocytosis of the insulin granules. We monitored $[Ca^{2+}]_i$ in wildtype and ClC-$3^{-/-}$ islets (Fig. 1E). Basal $[Ca^{2+}]_i$ levels were 88±6 nM and 106±15 nM in wildtype (n=7) and and ClC-$3^{-/-}$ (n=10) islets, respectively. Following stimulation with 15 mM glucose, $[Ca^{2+}]_i$ rose to a peak value of 419±52 nM and 452±29 nM in wildtype and ClC-$3^{-/-}$ islets. In both cases, this peak was followed by $[Ca^{2+}]$i oscillations due to bursts of Ca^{2+}-dependent action potentials. The addition of the sulfonylurea tolbutamide (0.1 mM) increased $[Ca^{2+}]_i$ similarly in wildtype and knockout islets and peak $[Ca^{2+}]_i$ averaged 414±47 nM and 458±39 nM, respectively. Thus, if anything $[Ca^{2+}]_i$ is higher in ClC-3-deficient than in wildtype islets. The suppression insulin secretion must therefore involve processes downstream of metabolic sensing, electrical activity and $[Ca^{2+}]_i$-signaling.

Defective exocytosis in ClC-3 null beta-cells

We next compared the exocytotic capacity of isolated wildtype and ClC$3^{-/-}$ β-cells. The β-cell identity was established by the presence of a voltage-gated Na^+-current that inactivated with a $V_{0.5}$ of ~ -100 mV (Olofsson et al., 2002). Exocytosis was elicited by trains of ten 500-ms depolarizations from -70 mV to 0 mV. In wildtype β-cells, exocytosis proceeded throughout the train stimulus (Fig. 2A). The capacitance increase per pulse decreased from an average of ~75 fF in response to the initial depolarization to a final value of 10 fF/pulse (Fig. 2B). The total capacitance increase of control cells averaged 381±36 fF (n=14). In ClC-3 KO β-cells, the capacitance increases per pulse were much smaller throughout the train (Fig. 2C-D), reaching a maximum rate of 20 fF/pulse with the total capacitance increase being a mere 70±12 fF ($P<0.001$ vs. control; n=14). The secretory response of β-cells lacking ClC-3 was

largely normalized by infecting the cells with a recombinant Semliki Forest Virus (SFV) encoding ClC-3 (Fig. 2E-F); the total capacitance increase averaging 259±18 fF (n=5; P<0.001 vs. ClC-3$^{-/-}$).

These findings corroborate the insulin release data (Fig. 1), and further suggest that the secretion defect is a cell-intrinsic consequence of the lack of ClC-3 and not due to systemic/paracrine effects. The latter conclusion is supported by RNAi-mediated silencing of ClC-3 in INS1 cells. Western blotting with densitometric analysis revealed that ClC-3 was reduced by ~70% within 72 h (Fig. 2G). This correlated with a 22±5% (P<0.01 silencer vs. control; Fig. 2H) inhibition of stimulated GH release (GH used as an insulin proxy to detect secretion in transfected cells (Ivarsson et al., 2005) and a marked 65% decrease (P<0.05 vs. control) in exocytosis elicited by trains of depolarization (Fig. 2I-J).

ClC-3 control of insulin granule acidification and priming

How does ablation of ClC-3 suppress exocytosis? We tested whether ClC-3 is important for granule priming. Exocytosis was elicited by an intracellular $[Ca^{2+}]_i$ dialysis protocol (1.5 μM free $[Ca^{2+}]_i$ with 3 mM Mg-ATP and 0.1 mM cAMP) (Fig. 3A). In wildtype β-cells, cell capacitance increased by 1.2±0.15 pF over 60 s, equivalent to the fusion of ~400 secretory granules (MacDonald et al., 2006). For comparison, exocytosis of the readily releasable pool (RRP) of primed insulin granules corresponds to a capacitance increase of only 0.1 pF or ~33 granules. The steady-state rate of capacitance increase provides an estimate of the rate of mobilization of new granules to the RRP, and averaged 20±2 fF/s (n=15). In ClC-3$^{-/-}$ β-cells, the rate of capacitance increase was limited to 12±1 fF/s (n=19; P< 0.01 vs WT). Thus, mobilization was reduced by ~40% in β-cells lacking ClC-3.

ClC-3 has been proposed to promote mobilization by providing a shunt conductance that allows the granule interior to acidify (Barg et al., 2001; Maritzen et al., 2008). In Fig. 3B we tested whether ablation of ClC-3 affects intragranular pH using the fluorescent probe LysoSensor Green DND-189 (LSG). The protonophore CCCP (0.1 mM) was introduced to the cytosol using a patch pipette. Addition of CCCP at t=0 led to a prompt reduction of fluorescence as the intragranular pH increased and fluorescent probe moved out of the cell. CCCP-mediated H^+-efflux from the granule is electrogenic. In the absence of a counter-ion, a large electrical potential will rapidly develop when the H^+ permeability is increased that would prevent pH equilibration across the granule membrane. If ClC-3 Cl^- channel activity is required for proton translocation over the granule membrane, then loss of these channels should reduce H^+-efflux via the protonophore leading to a reduced loss of fluorescence. Indeed, the CCCP-induced fluorescence decrease at steady-state (90 s after addition of CCCP) was reduced from 41±9% in wildtype cells to 18±5% in ClC-$3^{-/-}$ β-cells (*P <0.05). Thus, it appears that ClC-3 represent a quantitatively important shunt conductance in β-cell granules. The validity of LSG as a reporter of changes in intragranular pH was also verified (Supplemental Fig. 2).

Subcellular localization of ClC-3

Which acidic cellular compartments exhibit ClC-3-dependent pH-regulation? Earlier immunocytochemical data indicate that ClC-3 is present in membranes of insulin-containing secretory granules (Barg et al., 2001), but subsequent islet fractionations data suggest that the transporter is rather enriched in lighter (endosome/SLMV) fractions (Maritzen et al., 2008). To obtain a highly enriched fraction of insulin

granules, a fusion protein containing EGFP and phogrin, a highly selective marker of the LDCVs (Hutton, 1989), was expressed in insulin-secreting INS1 cells followed by immunoprecipitation using an antibody directed against EGFP (Varadi et al., 2005). Granules isolated by EGFP-labeling were enriched for insulin by a factor of ~20 over the homogenate when normalized to protein content. Similarly, this fraction contained significant ClC-3 immunoreactivity at levels that were >20-fold enriched above those in the homogenate, but did not exhibit immunoreactivity for markers of other membrane compartments (Fig. 3C). Confocal immunocytochemistry in single sorted granules demonstrated insulin immunoreactivity in >95% of the single granules that exhibited both EGFP and ClC-3 expression (n=26) (Fig. 3D). This finding was further substantiated by negative immuno EM of the sorted insulin granules, which demonstrated co-expression of ClC-3 in >80% of the granules (n >300) without noticeable unspecific background staining (Fig. 3E). Similar data wer also obtained by conventional immuno-EM (Supplemental Fig. 3).

Normal beta-cell ultrastructure in ClC-3 null mice

ClC-3 ablation did not interfere with granule biogenesis. Ultrastructural analyses revealed that the number of granules (total as well as docked) remained unchanged in ClC-$3^{-/-}$ islets. Moreover, their appearance and diameter were unaltered (Fig. 4A-D). The diameters averaged 333±8 (n=1638 granules; N=4 animals) and 329±8 nm (n=1279 granules; N=3 animals) in wildtype and ClC-$3^{-/-}$ β-cells, respectively. These findings suggest that insulin processing overall proceeds well in the absence of ClC-3, and agree with the marginal decrease in islet insulin content (Fig. 1B).

ClC-3 controls in vivo insulin secretion

To determine the systemic consequences of the ClC-3 deficiency on glucose homeostasis and insulin release, serum insulin and glucose concentrations were finally measured in wildtype and ClC-3$^{-/-}$ mice after an intraperitoneal glucose challenge (2g/kg body weight). Control mice responded to the glucose challenge with an increase in plasma insulin levels both at 3 and 8 min but no such response was detected in ClC-3 KO mice (Fig. 4E). Likewise, glibenclamide (500 µg/kg body weight), which in wildtype mice evoked a transient stimulation of insulin secretion, failed to enhance insulin secretion in ClC-3-deficient mice (Fig. 4F).

DISCUSSION

Secretory granules must undergo a priming reaction to gain release competence. We have previously proposed that priming of insulin granules requires the acidification of their lumen (Barg et al., 2001) and data in favor of this hypothesis have been reported (Stiernet et al., 2006). Previous evidence suggestive of a role of ClC-3 in insulin secretion involved immunoinhibition (Barg et al., 2001) and antisense approaches (Juhl et al., 2003) to suppress ClC-3. However, these procedures can always be questioned for the risk of unspecific effects. Here we have re-visited the role of ClC-3 in insulin secretion by analyzing mice in which these channels had been genetically removed. The new data presented here provide additional evidence that ClC-3 plays a role in insulin secretion.

The reduced insulin secretion capacity of ClC-3$^{-/-}$ β-cells is evident from the islet batch incubations (Fig. 1), as well as the reduced rates of replenishment of the readily releasable pool of granules in the Ca^{2+}-infusion experiments (Fig. 3).

Furthermore, in accordance with the notion that ClC-3 provides a shunt conductance required for granule acidification and priming, H^+-fluxes and priming were reduced by ~50% in ClC-$3^{-/-}$ β-cells (Fig. 3). However, the finding that these processes were not abolished argues that there exist additional mechanisms for granule priming/acidification in the β-cell. It is likely that these processes account for the normality of basal plasma insulin and glucose levels in the knockout animals. It is only when insulin secretion must increase much beyond basal that the demand of secretory granules exceeds that which can be met by the ClC-3-independent mechanisms.

It may seem surprising that the ClC-$3^{-/-}$ mouse is not overtly diabetic. However, it should be noted that they retain a certain degree of glucose-stimulated insulin secretion, which is a likely explanation for the relatively mild phenotype. In addition, only ~30% of glucose tolerance in mice is mediated by insulin and non-insulin-dependent mechanisms are significant (Pacini et al., 2001). We cannot entirely exclude the possibility that systemic effects due to the global knockout of ClC-3 contributes to the effect. However, this possibility seems less likely given the *in vitro* findings, e.g. that the effects of ClC-3 ablation on single-cell exocytosis can be reversed by infection of ClC-3. This conclusion is underpinned by the finding that siRNA-mediated downregulation of ClC-3 in INS1 cells is associated with a significant reduction of secretion.

We acknowledge that dense core granules (LDCVs) may not be the sole location of ClC-3. Indeed, the protein appears to enrich in neuronal synaptic vesicles (SVs) (Stobrawa et al., 2001), in endosomes and SLMVs of neuroendocrine PC12 cells

(Salazar et al., 2004), as well as in β-cells (Maritzen et al., 2008). However, the data presented here indicate that insulin granule membrane contains significant levels of ClC-3 (Fig. 3C-E). These data provide strong argument for a direct role of ClC-3 in β-cell exocytosis and in vivo insulin secretion. It is of interest that exocytosis in adrenal chromaffin cells was also reduced in the same $ClC3^{-/-}$ knockout mouse model (Maritzen et al., 2008), although the mechanisms involved were not examined in detail. Collectively, these findings raise the interesting possibility that ClC-3 may play a more general role in the priming and exocytosis of large dense core vesicles in endocrine cells.

RESEARCH DESIGN AND METHODS

Animals and in vivo experiments.

$ClC\text{-}3^{-/-}$ and $ClC\text{-}3^{+/+}$ littermates were used in these experiments. Details of the generation of the mice and their other characteristics have been summarized elsewhere (Stobrawa et al., 2001). The mice were generated in Hamburg and transported to Lund at least 2 weeks prior to the functional experiments.

Blood sampling in the in vivo experiments were conducted as described previously (Salehi et al., 1999). The surgical procedures used in the *in vitro* and *in vivo* studies were approved by the ethical committee at Lund University.

Isolation of islets and hormone release assays

For the static hormone release measurements, adult mice were killed by cervical dislocation, the pancreas quickly excised and pancreatic islets isolated by standard

collagenase digestion. Insulin and glucagon secretion were measured in a KRB-buffer as described previously (Salehi et al., 1999). Total insulin islet content was determined after extraction with acidic ethanol. Comparison of insulin/proinsulin release was made using a rat/mouse proinsulin and mouse insulin ELISAs (Mercodia, Uppsala, Sweden).

Imaging and electrophysiology

Electron microscopy and fura-2 measurements of $[Ca^{2+}]_i$ in intact islets were performed as described previously (Olofsson et al., 2002).

Capacitance recordings of single β-cell exocytosis were performed using the standard whole-cell technique and procedures described previously (Barg et al., 2001). The extracellular medium consisted of (in mM) 118 NaCl, 20 TEA-Cl, 5.6 KCl, 1.2 $MgCl_2$, 2.6 $CaCl_2$, 5 D-glucose and 5 HEPES (pH 7.4 with NaOH). The standard electrode (intracellular) solution contained (in mM) 125 Cs-glutamate, 10 KCl, 10 NaCl, 1$MgCl_2$, 5 HEPES, 0.05 EGTA, 3 Mg-ATP and 0.1 cAMP (pH 7.15 with KOH). In the experiments in Fig. 3A, glutamate was added as monopotassium salt and $[Ca^{2+}]_I$ was buffered to ~1.5 μM (cf. (Ivarsson et al., 2005)) by inclusion of 10 EGTA and 9 $CaCl_2$. For rescue experiments (Fig. 2 E-F), ClC-$3^{-/-}$ islets were infected with a ClC-3-encoding recombinant Semliki Forest Virus prior to dispersion into single cells and then cultured overnight.

Insulin granule fractionation and pH measurements

Granular pH was monitored semi-quantitatively as outlined elsewhere (Barg et al., 2001), using LysoSensor™Green DND-189® (5 μM; Molecular Probes). Insulin

granule-specificity of LSG fluorescence was evaluated using cells infected with an in-house IAPP-Cherry adenoviral construct. Granule fluorescence was visualized by total internal reflection fluorescence microscopy (Hoppa & Rorsman, manuscript under editorial consideration).

A highly enriched LDCV fraction was obtained by using a recombinant phogrin-EGFP adenovirus made using the BD Adeno-X expression system 1 (Clontech, CA, U.S.A). INS-1 cells were infected for 1 h and homogenized after 36 h culture. The post-nuclear supernatant was pelleted (5 000 × *g* for 15 min, 4^{o}C) and resuspended in a sorting buffer containing (in mM) 135 KCl, 10 NaCl, 1 $MgCl_2$, 5 Hepes, 2 EGTA (pH 7.15 with KOH) and 0.1% BSA. EGFP-positive particles were collected using a Becton Dickinson Cell Sorter (San Jose, CA) and tested for insulin and protein content (Fig. 3D). For immunostaining (Fig. 3E), the sorted granules were attached on polylysin-coated coverslips, followed by fixation, permeabilization and overnight incubation at 4^{o}C with guinea pig anti-insulin (1:100), and rabbit anti-ClC-3 (1:100) primary antibodies. After washing, the granules were incubated at 22^{o}C with donkey-raised secondary antibodies (Cy3-anti-guinea pig [1:400] and Cy-5-anti-rabbit [1:400]), and analysed using a Zeiss LSM 510 confocal microscope. Negative immuno EM was performed as previously outlined (Wiberg et al., 2001) using the same primary antibodies, coupled to 5-nm (insulin) or 25-nm (ClC-3) gold particles.

RNA-interference and GH-release in INS-1 cells

ClC-3 silencing was accomplished using the EGFP-containing $P^{RNA\text{-}H1.1}$ vector (GenScript Corp, Piscataway, NJ, U.S.A) with 76 basepair shRNA inserts. EGFP-expressing cells were collected 72 h-post-infection using a Becton Dickinson cell

sorter. Efficency of silencing was estimated by immunoblotting for ClC-3. The most efficient silencer construct (S3) contained the CTCCGGAATTCCAGAGATTAA target sequence in rat ClC-3 and was used for all functional assays.

hGH secretion was measured in INS-1 cells using 0.2 µg of the S3 silencer or scrambled control oligo inserted into the $P^{RNA\text{-}H1.1}$ vector, and 0.2 µg of the human GH-expressing vector, as previously detailed (Ivarsson et al., 2005).

Data are quoted as mean values ± S.E.M. of indicated number of experiments. Statistical significance was evaluated using Student's *t*-test.

References

al-Awqati, Q. (1995). Chloride channels of intracellular organelles. Curr Opin Cell Biol *7*, 504-508.

Barg, S., Huang, P., Eliasson, L., Nelson, D. J., Obermuller, S., Rorsman, P., Thevenod, F., and Renstrom, E. (2001). Priming of insulin granules for exocytosis by granular Cl(-) uptake and acidification. J Cell Sci *114*, 2145-2154.

Hara-Chikuma, M., Yang, B., Sonawane, N. D., Sasaki, S., Uchida, S., and Verkman, A. S. (2005). ClC-3 chloride channels facilitate endosomal acidification and chloride accumulation. J Biol Chem *280*, 1241-1247.

Hutton, J. C. (1989). The insulin secretory granule. Diabetologia *32*, 271-281.

Ivarsson, R., Jing, X., Waselle, L., Regazzi, R., and Renstrom, E. (2005). Myosin 5a controls insulin granule recruitment during late-phase secretion. Traffic (Copenhagen, Denmark) *6*, 1027-1035.

Juhl, K., Hoy, M., Olsen, H. L., Bokvist, K., Efanov, A. M., Hoffmann, E. K., and Gromada, J. (2003). cPLA2alpha-evoked formation of arachidonic acid and lysophospholipids is required for exocytosis in mouse pancreatic beta-cells. Am J Physiol Endocrinol Metab *285*, E73-81.

MacDonald, P. E., Braun, M., Galvanovskis, J., and Rorsman, P. (2006). Release of small transmitters through kiss-and-run fusion pores in rat pancreatic beta cells. Cell metabolism *4*, 283-290.

Maritzen, T., Keating, D. J., Neagoe, I., Zdebik, A. A., and Jentsch, T. J. (2008). Role of the vesicular chloride transporter ClC-3 in neuroendocrine tissue. The Journal of neuroscience *28*, 10587-10598.

Olofsson, C. S., Gopel, S. O., Barg, S., Galvanovskis, J., Ma, X., Salehi, A., Rorsman, P., and Eliasson, L. (2002). Fast insulin secretion reflects exocytosis of docked granules in mouse pancreatic B-cells. Pflugers Arch *444*, 43-51.

Pacini, G., Thomaseth, K., and Ahren, B. (2001). Contribution to glucose tolerance of insulin-independent vs. insulin-dependent mechanisms in mice. Am J Physiol Endocrinol Metab *281*, E693-703.

Piwon, N., Gunther, W., Schwake, M., Bosl, M. R., and Jentsch, T. J. (2000). ClC-5 Cl- -channel disruption impairs endocytosis in a mouse model for Dent's disease. Nature *408*, 369-373.

Rorsman, P., and Renstrom, E. (2003). Insulin granule dynamics in pancreatic beta cells. Diabetologia *46*, 1029-1045.

Salazar, G., Love, R., Styers, M. L., Werner, E., Peden, A., Rodriguez, S., Gearing, M., Wainer, B. H., and Faundez, V. (2004). AP-3-dependent mechanisms control the targeting of a chloride channel (ClC-3) in neuronal and non-neuronal cells. J Biol Chem *279*, 25430-25439.

Salehi, A., Chen, D., Hakanson, R., Nordin, G., and Lundquist, I. (1999). Gastrectomy induces impaired insulin and glucagon secretion: evidence for a gastro-insular axis in mice. J Physiol *514 (Pt 2)*, 579-591.

Sonawane, N. D., and Verkman, A. S. (2003). Determinants of [Cl-] in recycling and late endosomes and Golgi complex measured using fluorescent ligands. The Journal of cell biology *160*, 1129-1138.

Stiernet, P., Guiot, Y., Gilon, P., and Henquin, J. C. (2006). Glucose acutely decreases pH of secretory granules in mouse pancreatic islets. Mechanisms and influence on insulin secretion. The Journal of biological chemistry *281*, 22142-22151.

Stobrawa, S. M., Breiderhoff, T., Takamori, S., Engel, D., Schweizer, M., Zdebik, A. A., Bosl, M. R., Ruether, K., Jahn, H., Draguhn, A., *et al.* (2001). Disruption of ClC-3, a chloride

channel expressed on synaptic vesicles, leads to a loss of the hippocampus. Neuron *29*, 185-196.
Varadi, A., Tsuboi, T., and Rutter, G. A. (2005). Myosin Va transports dense core secretory vesicles in pancreatic MIN6 beta-cells. Molecular biology of the cell *16*, 2670-2680.
Wiberg, C., Hedbom, E., Khairullina, A., Lamande, S. R., Oldberg, A., Timpl, R., Morgelin, M., and Heinegard, D. (2001). Biglycan and decorin bind close to the n-terminal region of the collagen VI triple helix. The Journal of biological chemistry *276*, 18947-18952.
Yoshikawa, M., Uchida, S., Ezaki, J., Rai, T., Hayama, A., Kobayashi, K., Kida, Y., Noda, M., Koike, M., Uchiyama, Y., *et al.* (2002). CLC-3 deficiency leads to phenotypes similar to human neuronal ceroid lipofuscinosis. Genes Cells *7*, 597-605.

Acknowledgments

We thank Tanja Maritzen, Anselm A. Zdebik and Thomas J. Jentsch for breeding, genotyping, and supplying the mice used in this study. We also thank them for constructing and generously providing the Semliki forest viruses containing ClC-3 and control RNAs, as well as the anti-ClC-3 antibody before publication. We also thank Britt-Marie Nilsson for expert technical assistance. This work was made possible by grants from the Swedish Research Council (Linnaeus grant and project grants to E.R. and L.E.), the European Foundation for the Study of Diabetes (Europe-China Collaboration) supported by Bristol-Meyers-Squibb to D-Q.L., the Knut och Alice Wallenbergs Stiftelse (equipment), the NovoNordisk Foundation and the Wellcome Trust. E.R. and L.E. are Senior Researchers at the SRC.

Figure Legends

Figure 1. Effects of ClC-3 ablation on *in vitro* hormone release and intracellular calcium homeostasis. (**A**) Insulin secretion measured from wildtype (black) and ClC-$3^{-/-}$ islets (grey) in vitro during 1-h static incubations in the presence of 1 mM glucose, 1 mM glucose + 1 μM glibenclamide (G), 1 mM glucose at 50 mM extracellular K^+, 20 mM glucose and 20 mM glucose + 100 nM GLP-1 as indicated. (**B**) Islet insulin content from wildtype (black) and knockout (grey) islets. (**C**) As in (A) but insulin and proinsulin was measured at 1 and 20 mM glucose. (**D**) Ratio of insulin over proinsulin secretion in 20 mM glucose. Data are mean values ± S.E.M. of 9-23, 6-8 and 5-6 experiments (=animals) under the different conditions in A, B and C-D, respectively. ** P<0.01 *** P<0.001. (**E**) Intracellular $[Ca^{2+}]_i$ recordings in WT and ClC-$3^{-/-}$ islets. Glucose was increased from 5 mM to 15 mM and tolbutamide included in the medium as indicated. Data are representative for 7 (WT) and 10 (ClC-$3^{-/-}$) experiments.

Figure 2. Effects of ClC-3 ablation on regulated beta-cell exocytosis and secretion. (**A**) Increases in membrane capacitance (ΔC), evoked by a train of ten 500-ms voltage-clamp depolarisations from -70 mV to 0 mV (V) in a wildtype β-cell (identified by Na^+ current inactivation properties; cf. (34); inset). (**B**) Increases in membrane capacitance elicited by the individual pulses of the train stimulus (ΔC_n-ΔC_{n-1}). (**C-D**) Same as in (A-B) but using cells from ClC-$3^{-/-}$ mice. (**E-F**) Same as in (C-D) but ClC-3 had been reintroduced by Semliki Forest Virus. Data represent mean values ± S.E.M. obtained from 14, 14 and 5 cells in B, D and F, respectively. ***P < 0.001 **P < 0.01. (**G**) Silencing of ClC-3 demonstrated by Western blot analysis of

INS1 cells treated with vector-based RNAi against ClC-3 with either a scrambled control oligo (C) or silencing oligos S1-3. (**H**) Stimulated hGH secretion from control INS1 cells and cells in which ClC-3 had been down-regulated using S3. Data are mean values ± S.E.M. of 6 experiments. (**I**) Increases in membrane capacitance in ClC-3-silenced cells (gray bars) elicited by the individual pulses of the train stimulus (ΔC_n-ΔC_{n-1}). The black line shows data from control cells. (**J**) Total increase in ΔC (ΔC_{TOT}) in ClC-3-silenced cells (gray bar) and cells treated with a scrambled oligo (black bar). Data in (I-J) are mean values ±S.E.M. of 11 and 6 experiments, respectively. ** $P < 0.01$ and * $P < 0.01$.

Figure 3. **Expression of ClC-3 in isolated insulin granules and reduced granular proton permeability in ClC-3$^{-/-}$ β-cells.** (**A**) Exocytosis measured in wildtype (WT) and ClC-3$^{-/-}$ β-cells during intracellular dialysis with 1.5 μM $[Ca^{2+}]_i$. (**B**) Changes in granular pH following establishment of whole-cell configuration and wash-in of 0.1 mM CCCP in wildtype and ClC-3$^{-/-}$ β-cells. The whole-cell configuration was established at t=0. Data are given as mean fluorescence values normalized to fluorescence intensity at t=0 of 5 control cells and 9 ClC-3$^{-/-}$ cells. *P < 0.05. (**C**) Presence of ClC-3 in INS1 post-nuclear cell homogenates (HM), as well as enrichment in insulin-containing secretory granules (SG) purified by fluorescence activated "cell" sorting after tagging the vesicles with phogrin-EGFP. The same fractions were also tested for immunoreactivity against markers of plasma membrane (NaK ATPase), lysosomes (Cathepsin B), SLMVs (synaptophysin), early (Rab4) and recycling (Rab11) endosomes and mitochondria (Cytochrome C). (**D**) Confocal imaging of insulin and ClC-3 immunoreactivity in EGFP-tagged insulin granules. Scale bar 400 nm. (**E**) Negative immuno electromicrograph of an EGFP-tagged dense core granule, demonstrating co-expression of ClC-3 (25-nm gold particle) and insulin (5-nm particle), representative of >300 single granules studied.

Figure 4. Effects of ClC-3 ablation on β-cell ultrastucture and in vivo insulin secretion. (**A-B**) Typical electron micrographs of WT and ClC-3$^{-/-}$ β-cells. Total number (**C**), and number of granules docked with the plasma membrane (**D**) in wildtype and ClC-3-/-mice as indicated.. Data in (A-D) represent mean values ± S.E.M calculated from 3 and 4 animals per genotype. Scale bars 0.5 μm. (**E**) Changes in plasma glucose (upper) and plasma insulin concentration (lower) following an intraperitoneal glucose challenge. 2 g glucose/kg body weight was

administered at t=0. Serum insulin and glucose concentrations were measured before, and 3 and 8 min after injection. (**F**) Same as in (E) but insulin secretion was stimulated with glibenclamide (500 μg/kg body weight). Data in (E-F) are mean values ± S.E.M. from 12 wildtype and 13 ClC-3$^{-/-}$ mice in (E) and 7 wildtype and 8 ClC-3$^{-/-}$ mice in (F). **P<0.01.

[E] Figure 1
Click here to download high resolution image

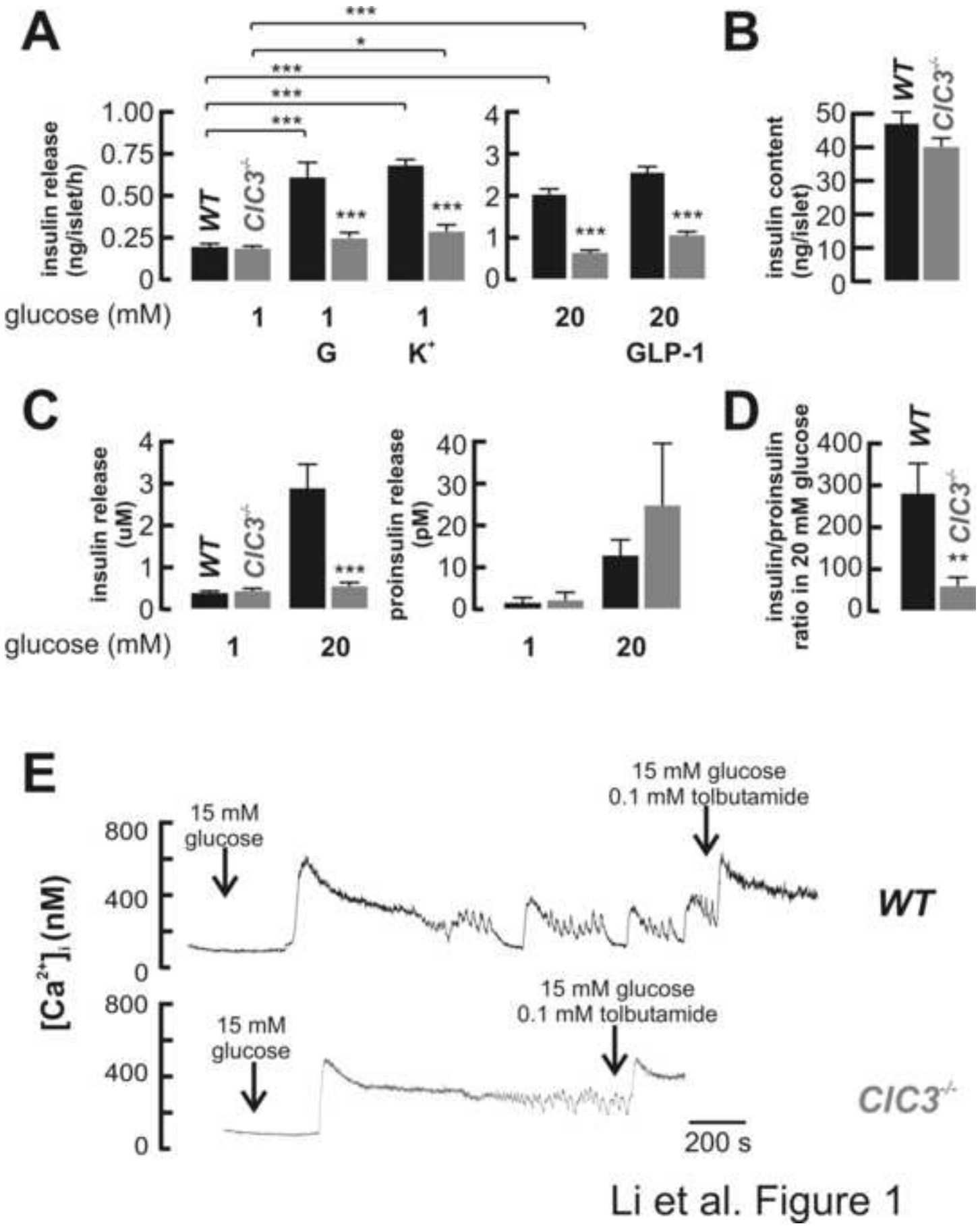

Li et al. Figure 1

[E] Figure 2
Click here to download high resolution image

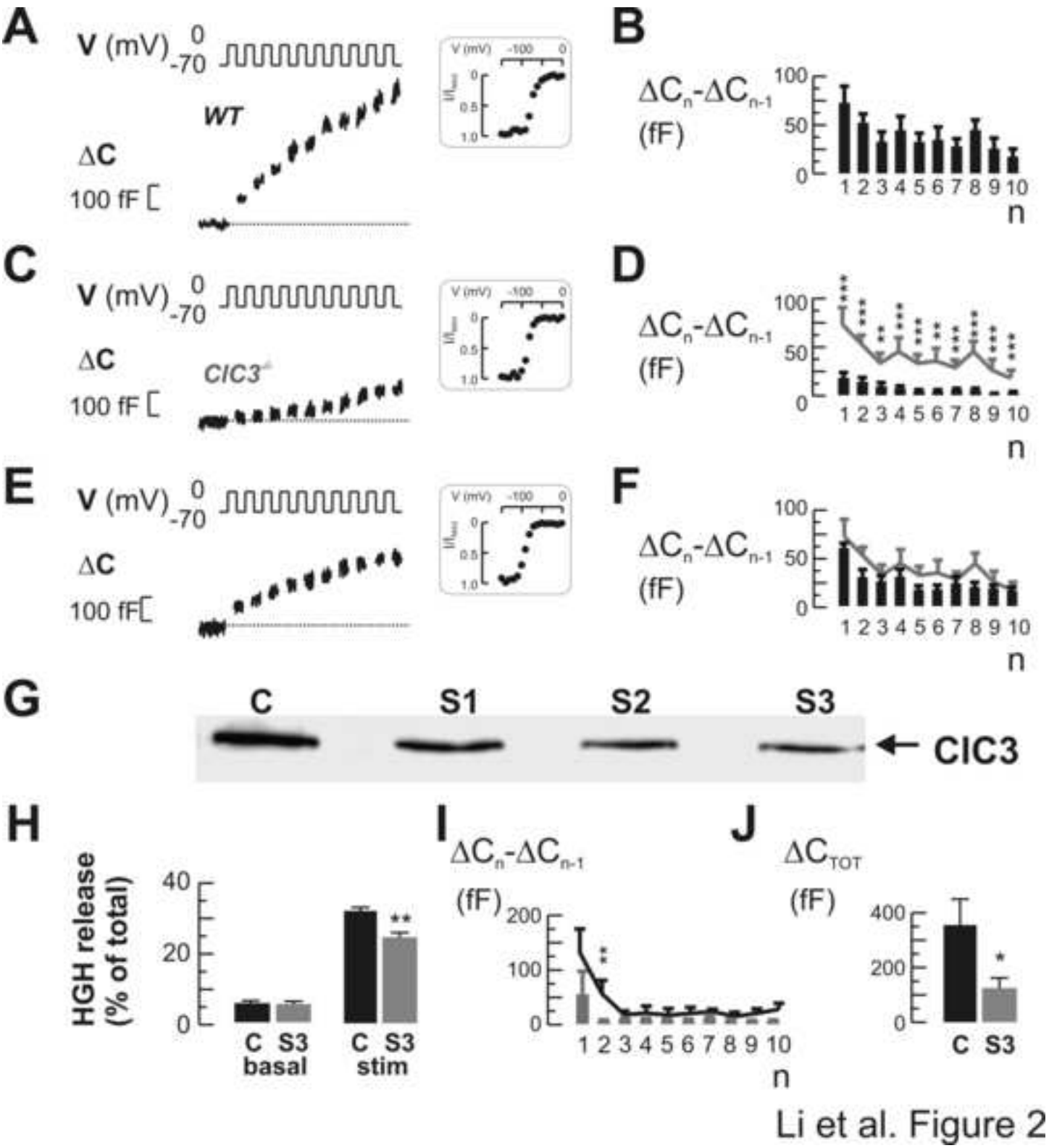

Li et al. Figure 2

[E] Figure 3
Click here to download high resolution image

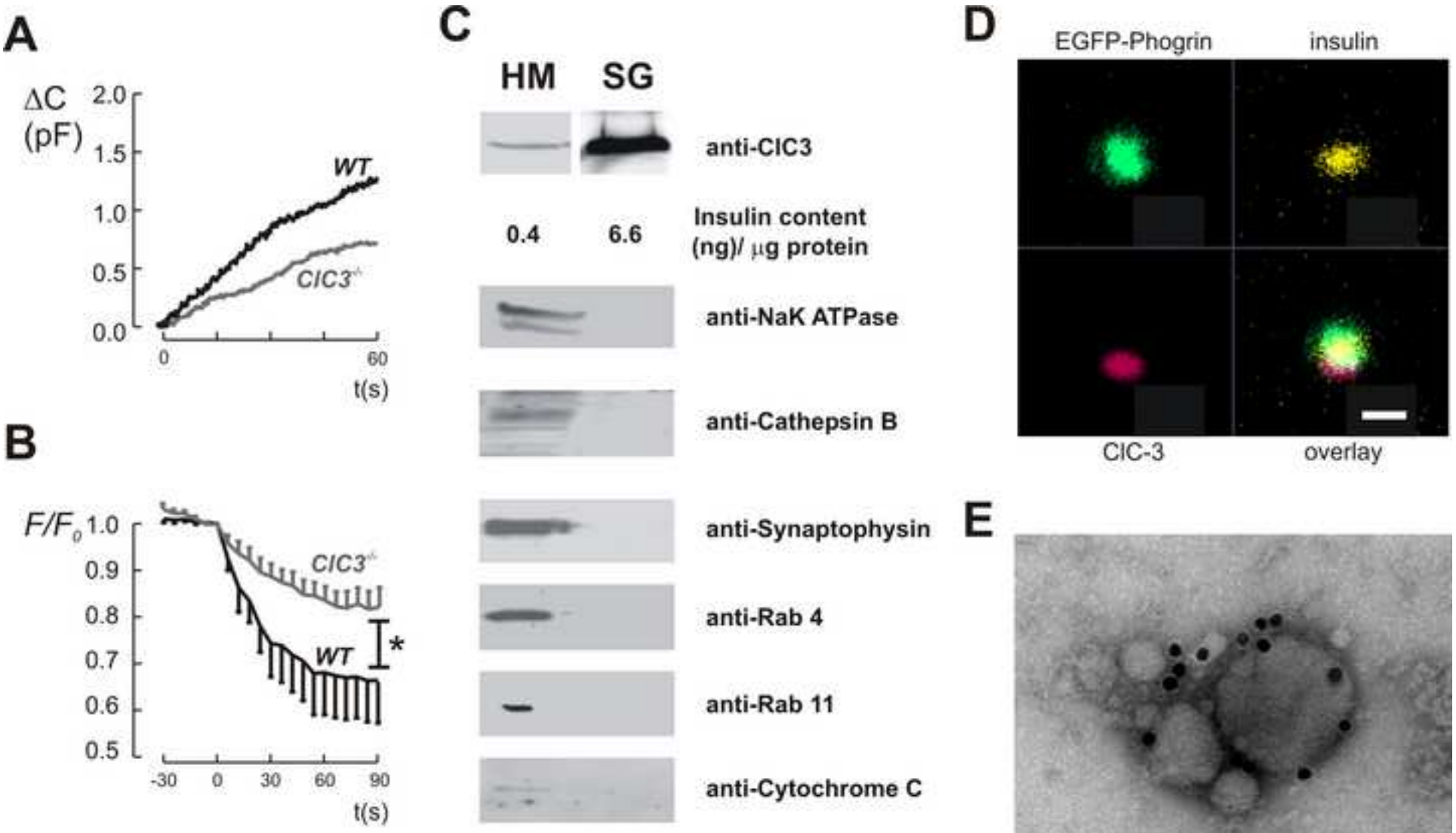

Li et al. Figure 3

[E] Figure 4

Click here to download high resolution image

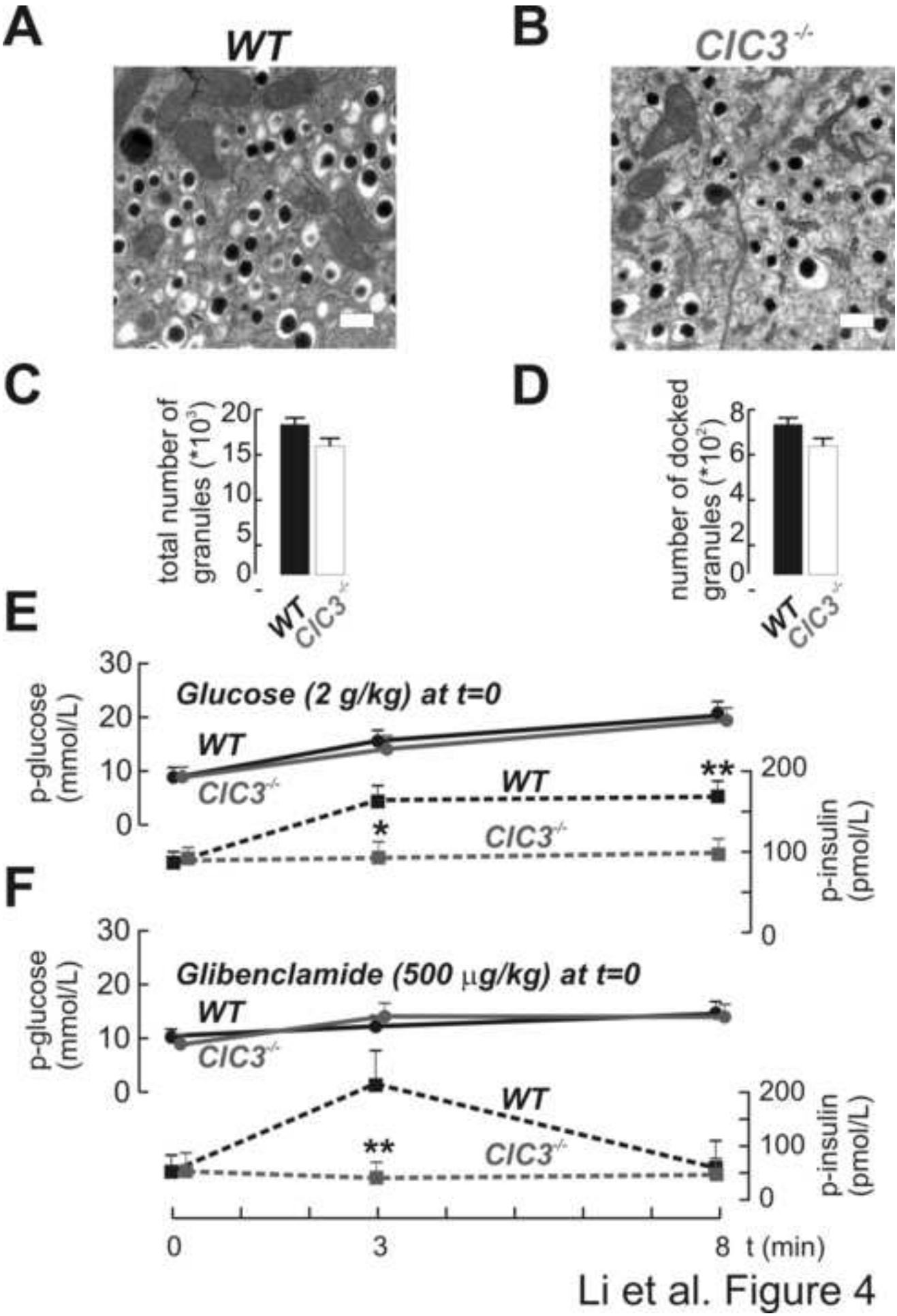

Li et al. Figure 4

Supplemental Data

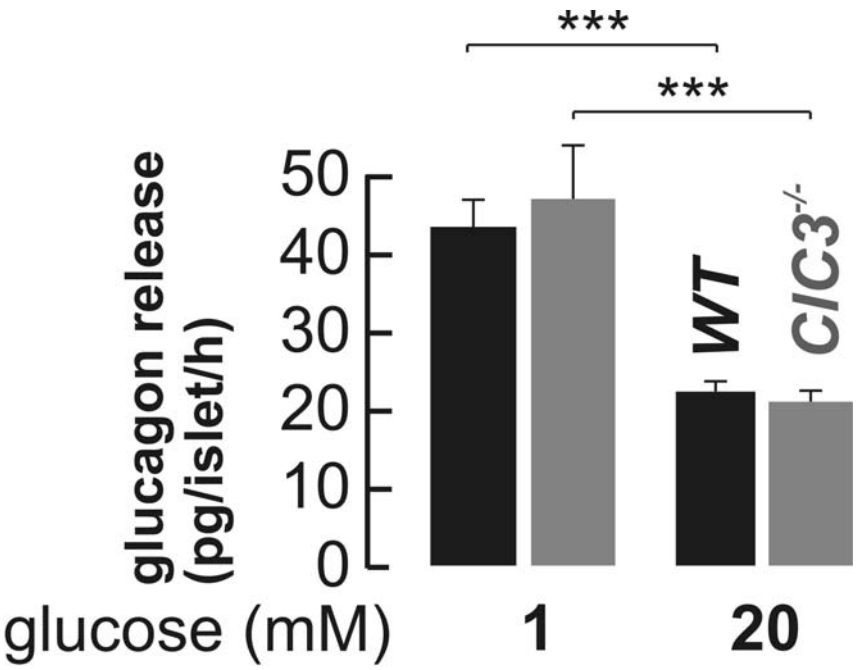

Li et al. Supplemental Figure 1

Supplemental Figure 1.

Glucagon secretion measured from wildtype (black) and ClC-3$^{-/-}$ islets (grey) in vitro during 1-h static incubations in the presence of 1 mM glucose or 20 mM glucose, as indicated.

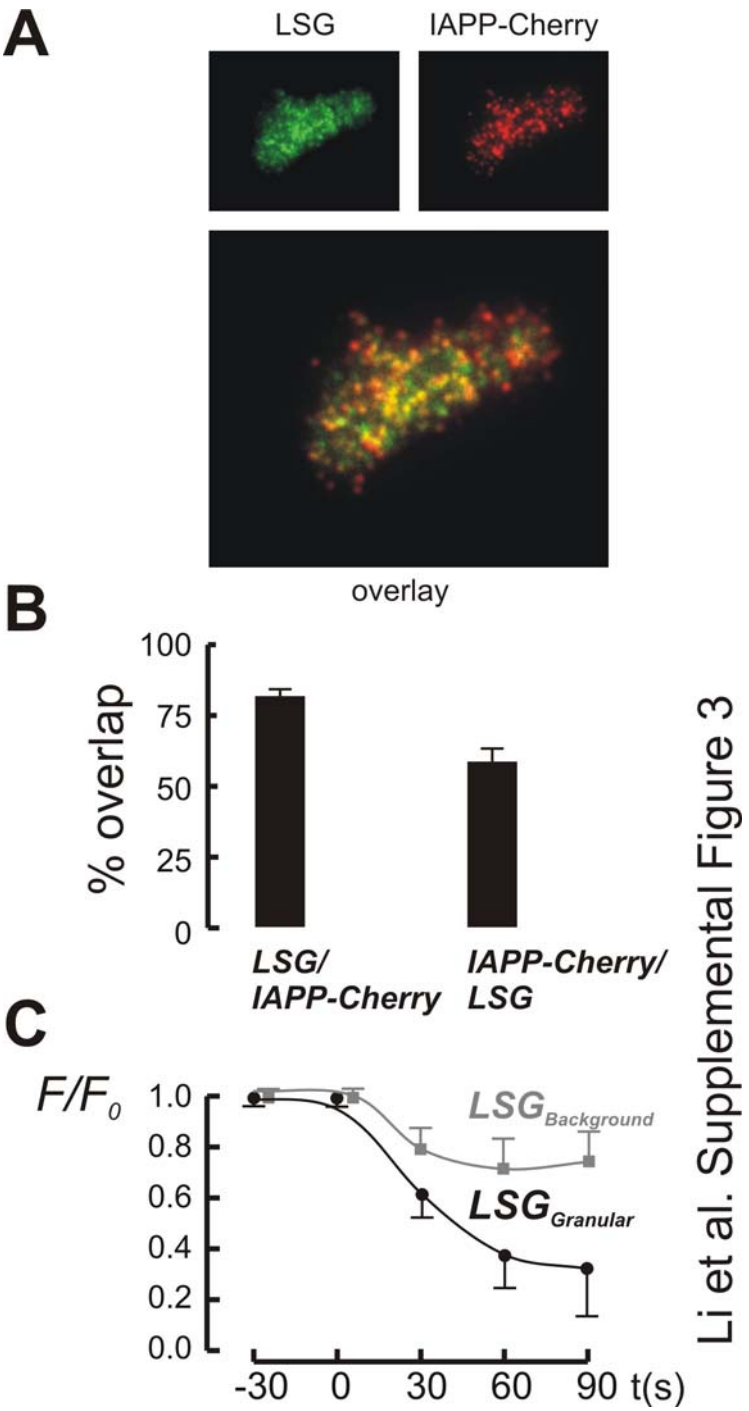

Supplemental Figure 2.

(**A**) Colocalization of LysoSensorGreen-DND-189 (LSG) fluorescence and insulin granule labelled by an adenoviral IAPP-Cherry construct (Vector BioLabs (Philadelphia, USA) and investigated by total internal reflection fluorescence (TIRF) microscopy. (**B**) Fraction (in %) of IAPP-Cherry-labelled granules exhibiting clear LSG fluorescence signals (LSG/IAPP-Cherry) and fraction of LSG-fluorescent

compartments expressiong IAPP-Cherry (IAPP-Cherry/LSG). Note that the 81% colocalization of LSG in IAPP-Cherry-tagged granules is similar to that of insulin (~80%, Hoppa and Rorsman, under editorial consideration). (**C**) CCCP-induced decreases in LSG fluorescence are ~3-fold more pronounced in the granular compartment ($LSG_{Granular}$) than in non-granular locations ($LSG_{Background}$). Data in (B) and (C) are expressed as mean values ± S.E.M. and are from 6 cells.

TIRF imaging was done using an Olympus IX-81 microscope equipped with a 150x/1.45 Apo lens (Olympus, UK). LSG and IAPP-Cherry were excited using the 488 nm and the 561-nm lines of a diode laser (Point Source, UK), and emitted light was collected using a CCD camera (Cascade II 512B, Roper Scientific, Trenton, USA). Colocalization analysis was performed using Metamorph software (Molecular Devices, USA).

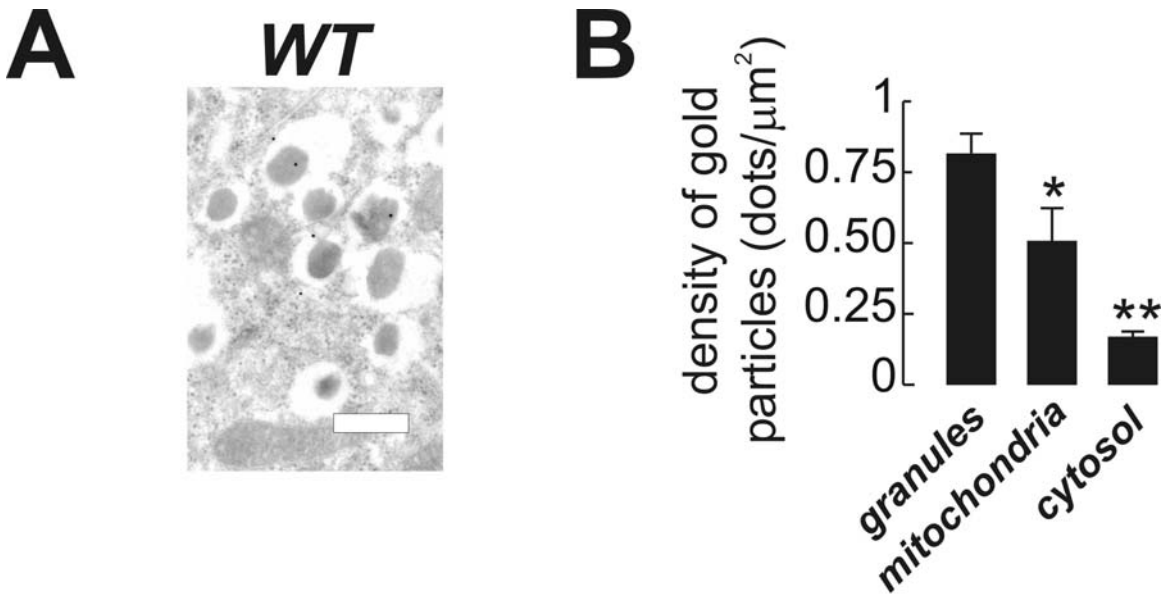

Li et al. Supplemental Figure 3

Supplemental Figure 3.

(**A**) Immunogold labelling of ClC-3 in a WT β-cell (**B**) Gold particle density in different subcellular compartments. Data represent mean values ± S.E.M calculated from 3 and 4 animals per genotype. Scale bar 0.5 μm.